20th International Conference on Structural Mechanics in Reactor Technology (SMiRT 20)
Espoo, Finland, August 9-14, 2009
SMiRT 20-Division-II, Paper 1861

Ratcheting-Fatigue Failure of Pressurized Elbows made of Carbon Steel

Suneel K Gupta , Sumit Goyal, Vivek Bhasin, K. K. Vaze, A.K. Ghosh and H. S. Kushwaha

Reactor Safety Division, Bhabha Atomic Research Center, Mumbai, 400085, India
e-mail: suneelkg@barc.gov.in

Keywords: Ratcheting, fatigue, cyclic loading, ratchet-strain, LCF life, pipe-elbow.

1 ABSTRACT

Ratcheting-fatigue investigations have been carried out to understand the ratcheting-fatigue failure of carbon manganese steel (conforming to ASME specification of SA-333 Gr.6). Experiments have been conducted on pressurized pipe-elbow assembly subjected to reversible cyclic bending, to assess the failure mechanics owing to ratcheting-fatigue synergy. These studies are required to evaluate the piping seismic design rules. These investigations have shown significant influence of the ratchet strain and non-relaxing mean stress on the low cycle fatigue life of material.

2 INTRODUCTION

Failure resistant design of any structure or component has always been the main aim of designer. The earthquake load, a main design basis accident loading, is considered in the design of the Nuclear Power Plant (NPP) structures as well as piping system. During large magnitude earthquake events, the pressurized elbows can experience inelastic cyclic excursions and can lead to accumulation of plastic strains, known as ratcheting. In past, a number of investigators like Ohno et. al. (1986), Chaboche et. al. (1991), Hasan et. al. (1992), Bari et. al. (2000) and Rahman et. al. (2008) etc. have been carried out investigations to understand the cyclic plasticity and ratcheting behavior of materials. However, they have concentrated mainly on material ratcheting behavior and its constitutive modeling but the ratcheting-fatigue interaction has not been addressed. However, some investigators like Boussaa (1994), Xia (1996), and Weib (2004) etc. has shown significant influence of interaction on fatigue life of component. To assess the structural integrity under ratcheting-fatigue, few researchers like Yahiaoui (1996) and Touble (1999) have carried out experimental and analytical investigations. Their investigations have led to changes in piping seismic design rules of various design codes. However, still there are a lot of unresolved issues related to the failure mechanism.

The elbows, among other piping components, exhibit highly strained regions in the piping system because of their high flexibility and are vulnerable to failure by ratcheting-fatigue. Therefore, to understand the ratcheting-fatigue failure mechanism, total eight numbers of ratcheting experiments were conducted on 8” NB Sch.100 size pipe-elbow assemblies of carbon steel. These tests were conducted under different combinations of constant internal pressure and large amplitude (quasi static) reversible cyclic displacement controlled loading.

In all these tests, there was significant accumulation of ratchet strain over a number of applied cycles along with presence of non-relaxing internal pressure stress and led to very early fatigue crack initiation in the component. In view of this, it is instructive to address the influence of ratcheting strain and pressure stress on fatigue behaviour. To understand the phenomena, a series of uniaxial ratcheting-fatigue experiments at specimen level have also been performed.

The analytical prediction of ratcheting needs modeling of cyclic plasticity response, which is quite complex. Therefore, to understand the analytical modelling aspects of ratcheting phenomenon, testing was followed by analytical assessment using the finite element analysis. Further, number of cycle to fatigue crack initiation were also evaluated using various available strain-life equations and compared with the experimental results.

3 FATIGUE-RATCHETING TEST DETAILS AND RESULTS

3.1 Test Description: Geometry and Material

Quasi static cyclic tests have been carried out on right angle large radius elbows of 219 mm outer diameter and 15 mm thickness. Its material conforms to specification of Primary Heat Transport (PHT) piping of Indian Pressurised Heavy Water Reactor (PHWR) and is equivalent to ASME specification of SA-333 Gr.6. The tensile properties of pipe material, that is, yield stress, tensile strength and Young's modulus is 288 MPa, 420 MPa and 203 Gpa respectively. Each elbow has been grid marked in axial direction (12 divisions) and circumferential direction (24 divisions) and thickness was measured at each grid point. It has been noticed that there is thickness variation of ±14% with respect to average thickness. In addition to this, diameter and bend radius have been measured. Eight number of Elbow Ratcheting Tests (ERT1-ERT8) have been conducted on the pressurised pipe-elbow assembly. The geometric details of test elbows have been given in Table 1.

Table 1: Geometry details of pipe-elbow specimens

Test Name	ERT1	ERT2	ERT3	ERT4	ERT5	ERT6	ERT7	ERT8
Outer Diameter (mm)	219	219	219	219	219	219	219	219
Average Thickness (mm)	15	15.1	15.1	15	15.1	14.8	14.9	15
Thickness at Crown (mm) (2 crown along circumference)	-	14.7	14.9	15	14.8	14.6	14.6	15.0
	-	15.7	15.4	15	14.8	14.6	15.1	15.1
Thickness at Intrados (mm)	-	16.9	17	17.2	17.2	16.6	17.1	16.7
Thickness at Extrados (mm)	-	14	13.9	13.2	13.2	13.2	12.7	13.1

3.2 Test Setup / Procedure

Straight pipe of 668 mm length (≈3D where D is the outer diameter of elbow) is welded at both the ends of the elbow in order to include the boundary effects that is, stiffening against ovalization due to connect piping. One end is fixed and the other end is connected with hydraulic actuator jack. The experimental setup of pipe-elbow assembly and instrumentation details used in ratcheting-fatigue test are shown in Fig. 1.

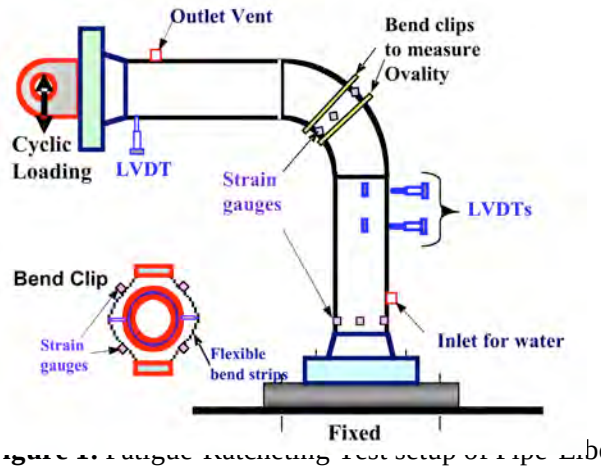

Figure 1. Fatigue ratcheting test setup of Pipe-Elbow assembly with various instrumentation used in test.

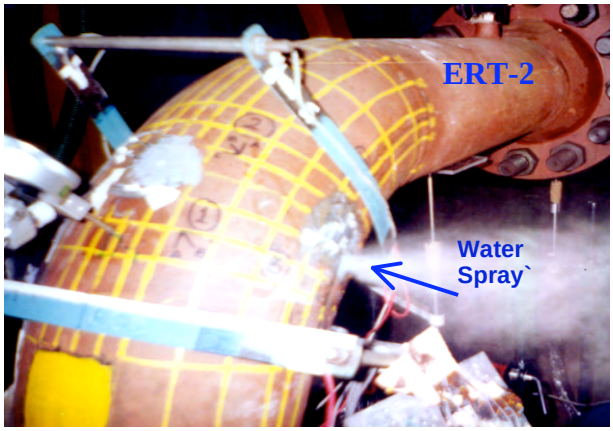

Figure 2. Axial through wall crack with water spray in ERT2 pipe-elbow assembly

The test instrumentation consists of a load cell, displacement transducers, strain gauges, bend clips, pressure gauge etc. The post yield strain gauge was used for strain measurements at crown, intrados, and extrados and near the fix end on the connected pipe. A set of bend clip gauges, as shown in Fig. 1, was used for crown-to-crown and intrados-to-extrados diametrical change measurements. In addition, the crack initiation event (except in ERT1-3) is also detected using online Acoustic Emission Technique (AET) and offline (holding test after few cycles) Ultrasonic Testing (UT) scanning. The AET signal were collected on line and treated as qualitative indicator for crack initiation event. The UT scanning was carried out for confirming these indications. In addition the experiment was paused, irrespective of AET indications after every 10 cycles for UT scanning.

Prior to the ratcheting-fatigue test, a trial test of 5 cycles each of ±5 mm displacement load with and without pressure was performed. This was done to determine the stiffness of elbow assembly and to ensure the response of various sensor/instrument. The trial test results are also used to validate the elastic stiffness and boundary conditions required for finite element model.

After the initial trial testing the elbow assembly was pressurized to a constant test pressure and then subjected to large amplitude reversible cyclic displacement controlled loading at the free end. The pressure was kept constant during a block of cyclic displacement loading. The pressure applied in different tests ranges from 120 bar to 300 bar which generates nominal hoop stress as $1/3\sigma_y$ to $2/3\sigma_y$. The displacement is applied in both closing and opening direction. Magnitude of displacement amplitude is taken such that the corresponding pseudo linear bending moment (calculated based on the elastic stiffness of pressurised pipe elbow test setup) ranges from 0.9 to 1.9 times of $M_{collpase}$ (collapse moment based on flow stress). This loading leads to equivalent pseudo linear stress amplitude (as per ASME Section III equation 9 with B'_2 index) of about $1.3\sigma_y$ to $3\sigma_y$ (or $2.7S_m$ to $6.2S_m$). These limits have been selected to develop criteria for ratcheting-fatigue failure and to evaluate the realistic safety margins available vis-a`-vis the new design rules. In design rule the moment and the stress used are pseudo elastic and evaluated by assuming material elastic behaviour. The Table 2 gives the test matrix, input loading details as well as the response load reactions, number of cycles in which the crack initiated and cycles when the elbows have failed under given loading. The failure occurs when initiated crack grows to through wall and results in water leakage.

Table 2: Details of the fatigue ratcheting tests conducted on pressurized pipe elbow

Test name	Internal Pressure (MPa)	Bending loading				Number of cycles			Average Ovalization / % Diameter Increase
		Applied LLD mm		Typical Reactions kN		Applied in blocks	Total Till failure	Crack initiation using AET /UT	
		Closing	Opening	Closing	Opening				
ERT1	12	-50	50	-80	88	3	339	--	7
		-55	55	-77	100	39			
	20	-51	79	-83	111	31			
		-50	75	-85	105	129			
	25	-50	75	-87	108.3	137			
ERT2	25	-91	44	-71	85	1	184	--	7
		-81	43	-83	101	5			
		-88	42	-97	115	178			
ERT3	30#	-84	42	-99	114	123	123	--	9
ERT4	30	-110	25	-108	113	94	94	30	10.5
ERT5	30	-61	25	-84.3	69.2	5	282	60	11.3
		-56	25	-85.8	70.4	2			
		-51	25	-82.6	68.7	1			
		-43	25	-85.6	61.3	194			
		-101	30	-109.1	113.1	80			
ERT6	25	-66	65	-145	165	62	62	35	13.1
ERT7	18.5	-50	50	-126	130	87*	87*	55	
ERT8	21.0	29	29	-101	83	675*	675*	210	6.8

*Note: * Failed at weld joint between the elbow and fixed end pipe.*

 # Pressure make up system failed in 70th cycles. In subsequent cycles there was steady pressure drop due to ratcheting and at failure the pressure was 25 MPa. ERT-4 is the repeated with same pressure as in ERT3.

3.3 Test Results and interpretation

Among the eight tests, in six of them the elbows have failed, following an appearance of a through wall axial crack, near the crown location. There was significant ballooning (7-13% increase in diameter), with simultaneous fatigue damage followed by crack initiation on inside surface at crown location and it grows till it becomes through wall thickness (Fig.2). Although the fatigue crack initiation took place on both side flank/crown, however it becomes through wall on one of the side. The through wall crack is nearly 100 mm axially oriented and 3-4^o down from crown towards intrados. In other two tests there was crack initiation too

at the crown of the elbow but simultaneously a crack appeared at the weld between elbow and vertical pipe and this crack grew to become through wall.

The same tested elbow (ERT2) has been cut to see the interior (ID surface) of crown (other side where crack does not grow to through wall). It is found that there was multiple crack initiation with axial orientation. One of the cracks in this piece has been used to calibrate the 45° angle probe pulse-echo UT instrument to confirm initiation. The same calibrated UT has been used for crack initiation detection in subsequent tests. From the Table 2, it can be observed that crack initiation (N_i) has taken place in 30 to 210 cycles however, final failure (N_f) in 62 to 625 cycles. Moreover, N_f and N_i depends upon the pressure and cyclic loading amplitudes.

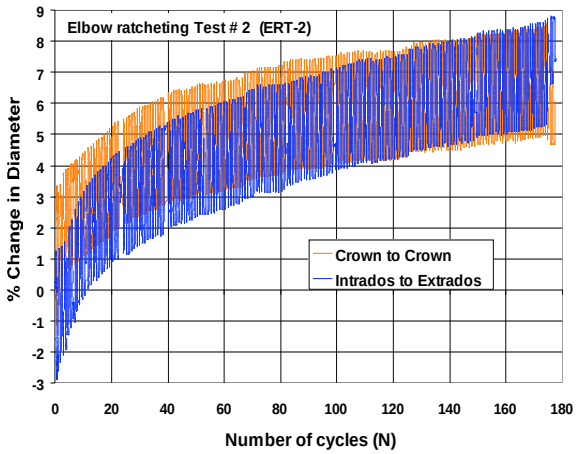

Figure 3. Plot of change in diameter (%) versus Cycles for ERT-2 test

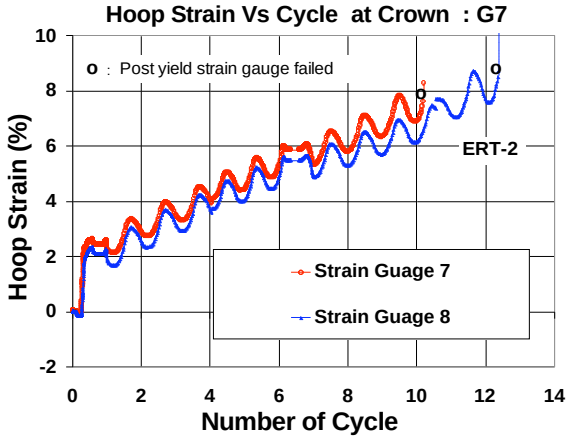

Figure 4. Plot of hoop strain (%) at crown versus number of load cycles for ERT-2 test

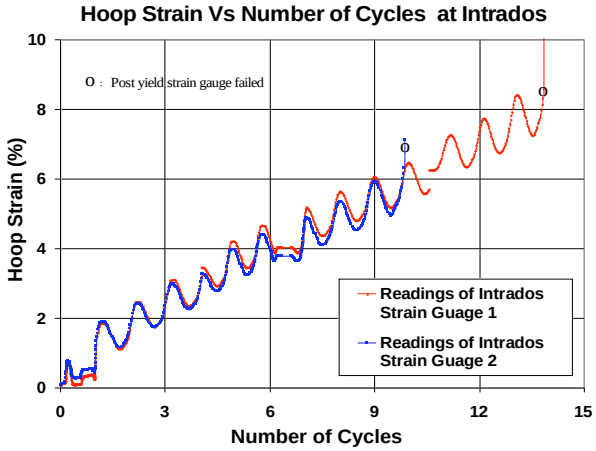

Figure 5. Hoop strain (%) at Intrados versus loading cycles for ERT-2 Test

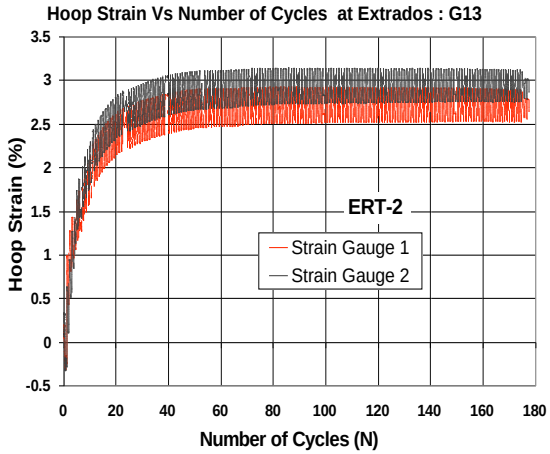

Figure 6. Plot of hoop strain (%) at extrados versus number of load cycles for ERT-2 test

Fig.3 shows the percentage increase in the crown to crown and extrados to intrados diameter with the number of cycle of loading for the ERT2 test. This curve measures the gross dilation/ballooning (that is, gross ratchet strain accumulation in hoop direction) in the elbow 45° section when subjected to high amplitude cyclic load under constant internal pressure. Similar results were obtained for other tests also and the final value is reported in the Table 2. Fig. 4 to 6 shows the typical (for ERT2) hoop strain versus number of load cycles at crown, intrados and extrados location respectively. The crown and intrados shows continuous ratcheting stain accumulation, however at extrados strain accumulation ceases in few cycles owing to plastic shakedown and subsequent response is plastic cycling.

The elbow ratchteing test also shows that the gross ballooning in initial 10 cycles is quite small in comparison to local strain accumulation at crown and intrados locations. In initial 10 cycles, gross ballooning is observed in a range of 1 % to 4% however, local strain accumulation at crown is in a range of 2% to 8%. It is important to notice that the cyclic strain amplitude at crown, in different tests, ranges from 0.5% to 1%. From the classical LCF curve it can clearly shown that strain cycling of such amplitudes could not lead to crack initiation and to failure in such small number of cycles (Table 2). These tests clearly points

out to significant interaction of ratchet strain (local accumulation strain) and sustained non-relaxing pressure stress with the LCF life.

In past, many investigators like Manson (1981), Xia Z (1996) and Lin (2000) have shown that the presence of ratchet strain and positive mean stress accelerate the fatigue damage and hence reduces the low cycle fatigue life. In general the effect of mean stress may not be significant for LCF tests under strain controlled cycling due to its relaxation in few cycles because of yielding of material. But during the pipe-elbow ratcheting tests, significant primary hoop stress will always be present at crown due to sustained pressure loading and will never relax to zero due to strain cycling (or displacement loading). Hence this will lead to reduction in LCF life. Secondly, the LCF life primarily depends on the fatigue ductility of the material. The accumulation of ratchet strain leads to reduction in fatigue ductility and so LCF life. This has also been investigated through a systematic uniaxial ratcheting and post ratchet LCF test and have been discussed in section 5.0.

4 RATCHETING-FATIGUE ANALYSIS

4.1 Finite Element Analysis

The results from these tests have been used to study the analytical modelling aspects of ratcheting phenomenon. Due to symmetry only half of the pipe-elbow assembly was modelled using 20 noded solid elements. To simulate the boundary conditions of test, the nodes at the bottom location were fixed for all degrees of freedom and symmetric boundary conditions were applied on the symmetry plane of cross-section. Then internal pressure with constant magnitude was applied to the elbow-pipe assembly. The axial pressure equivalent to longitudinal stresses was applied on the free end cross-section of the elbow. The displacement loading were applied to simulate the in-plane closing and opening. The finite element mesh has been shown in Fig.7.

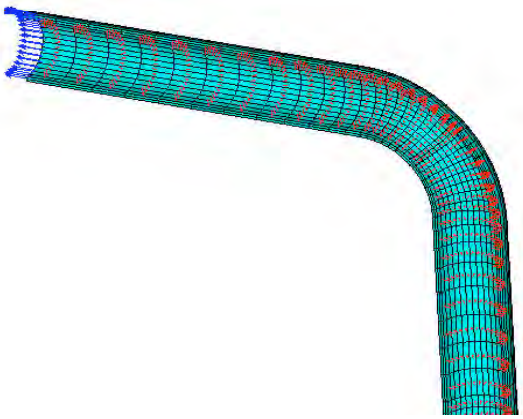

Figure 7. Finite element mesh for the Pipe-Elbow assembly in the fatigue ratcheting test (ERT5).

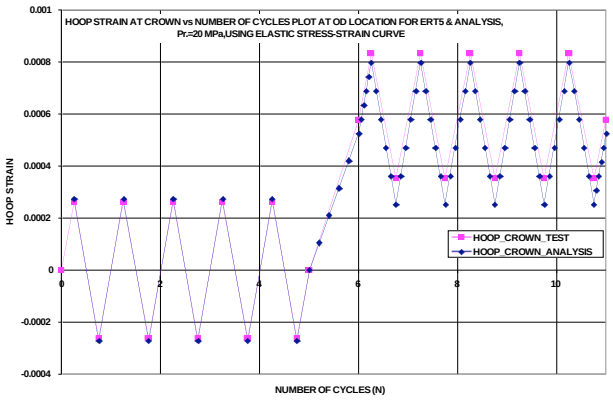

Figure 8. Comparison of FEM(elastic analysis)and trial test measured hoop strain at crown location.

Initially, linear elastic finite element analysis (FEA) was performed by applying trial test displacement loading. Strain at various locations were evaluated and compared with the corresponding test measured. Fig.8 shows the hoop strain comparison at crown location and it found in good agreement. This validated FE model was further used for ratcheting analysis which uses complex cyclic plasticity material models.

Modelling of cyclic plasticity response (kinematic hardening, cyclic hardening /softening etc.) is important for ratchet response prediction. However, idealised kinematic hardening models that is, Chaboche three-decomposed has been used in present ratcheting analysis. The Chaboche 3-decomposed model constants were evaluated for the stable hysteresis loop of reasonable strain range (±1%). With it, two cases were considered for the multilinear kinematic hardening law, in one case the unstabilised (monotonic) material stress-strain curve was used and for the other the stabilised (cyclic) material stress-strain curve was given as input in the analysis and also shown in Fig. 9. The material under consideration shows complex behaviour under cyclic loading when compared with monotonic. It exhibits mix response that is, cyclic softening response up to about 0.5% and hardening response beyond 0.5% strain.

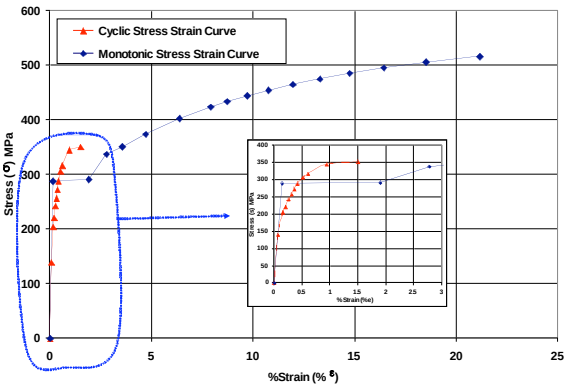

Figure 9. Monotonic and Cyclic stress curve of material (SA333 Gr.6)

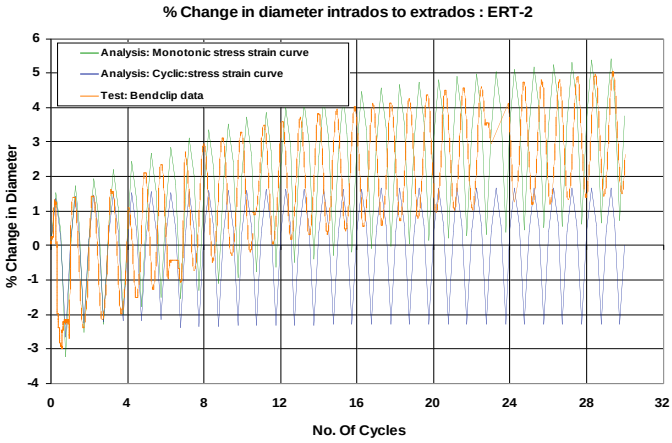

Figure 10. Comparison of test and finite element evaluated % change in crown to crown diameter vs. cycles history using different material models for ERT-5

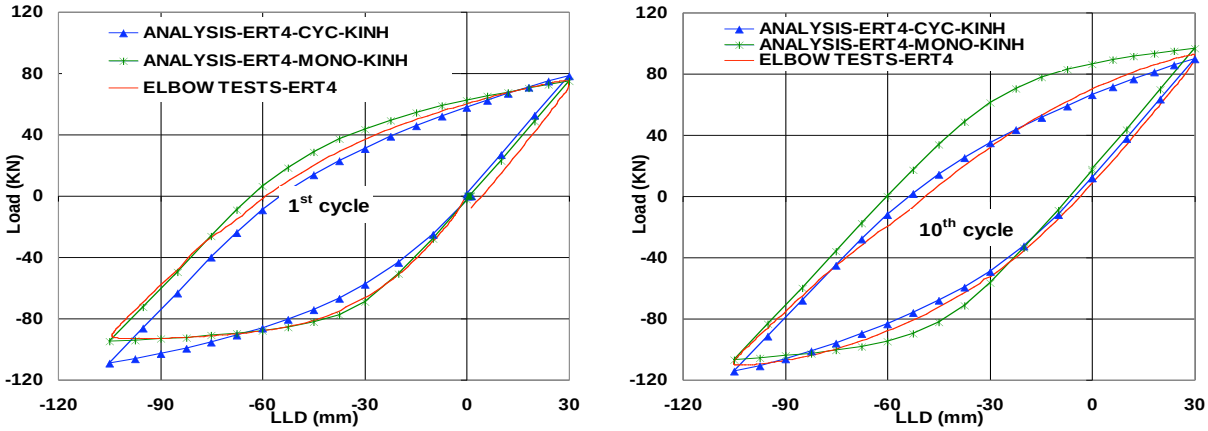

Figure 11. Comparisons of experimental Load vs. Load line Displacement for 1st cycle and 10th loading cycle results with FE analyses using monotonic and cyclic stress-strain curve for ERT-4 Tests.

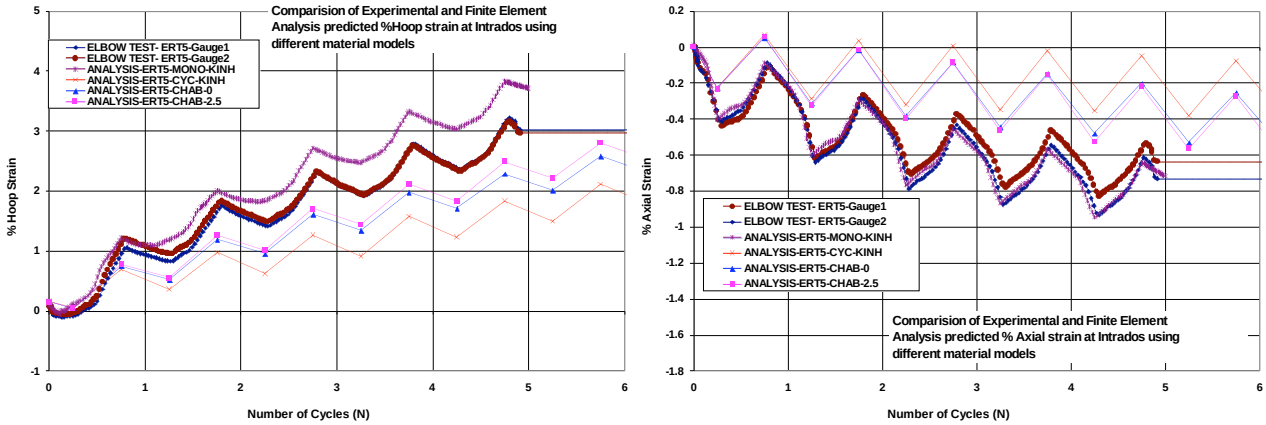

Figure 12. Comparisons of experimental hoop strain and axial strain at intrados vs. cycle history with FE analysis using different material models for ERT-5.

Finite element analysis has been performed with above discussed material models for ERT5, ERT4 and ERT2 tests. The load versus load line displacement (Load-LLD), gross dilation or change in diameter and the strains at various locations have been recorded in finite element analyses for all the material models considered and compared with the experimental results. Fig.10 to 12 show typical finite element results along with their comparison with the corresponding quantities recorded during the test.

It is observed that the test measured Load-LLD response for the 1st cycle is closely simulated by the analyses with monotonic (unstabilised) stress strain curve while 10th cycle onwards, test measured Load-

LLD response becomes close to the analyses with cyclic (stabilized) stress strain curve. This clearly demonstrates and validates the shift of the material's response (σ-ε curve) from monotonic to cyclic as results of cyclic loading. This point-out that the transition of the material's response (σ-ε curve) from monotonic to cyclic should be considered in modelling in order to simulated complete test response.

4.2 Crack Initiation Calculations

The crack initiation in these experiments has been tracked by on line AET and off line UT scanning of near by crown region. The crack initiation cycles (N_i) observed in the experiment ranges from 30 to 210 cycles (Table 2). As discussed in section 3.3, there is significant interaction of ratchet strain and sustained non-relaxing pressure stress with the Low Cycle Fatigue (LCF) damage. This aspect was investigated vis-à-vis different strain-life equations available for LCF damage assessment.

ERT4 case was selected for detailed crack initiation calculation since it took minimum number of cycles (N_i =30) for crack initiation. Therefore, detailed elastic-plastic 3D finite element analyses have been performed for loading history of initial 30 cycles only. From FEM analysis of ERT4, the time history of hoop strain and hoop stress was recorded at critical location (near crown) for 30 cycles. It was observed that the resulting strain amplitude varies with cycles as well as the mean strain keeps accumulating. Initially, mean hoop stress is small and increases with cycles till it reaches close to nominal hoop stress. The typical values of variations of various quantities such as hoop strain range ($\Delta\varepsilon_H$), hoop stress (σ_{mH}), triaxiality factor (q) (ratio of hydrostatic to von-mises stress) and accumulated hoop strain (ε_r) with cycles have been reported in Table 3. The damage calculation was carried out cycle by cycle and Miner's linear rule was used to obtain cumulative damage fraction and evaluated number of cycles for crack initiation.

Table.3: The variations of various stress / strain parameters with cycles at crown for ERT4

Cycle No. (N)	**N=2**	**N=5**	**N=10**	**N=20**	**N=30**
Strain range $\Delta\varepsilon_H$ (%)	1.75	1.98	2.02	2.3	2.37
Mean Hoop stress σ_{mH} (MPa)	46.82	107.12	145.47	173.89	187.38
Triaxiality factor $q=\sigma_h/\sigma_{eff}$	0.55	0.62	0.65	0.66	0.66
Accumulated Strain ε_r (%)	2.27	4.78	6.84	8.9	10.17

Fatigue crack initiation calculations have been made for ERT4 using following different strain-life equation available in literature. Summary of the different strain-life equation used for this study and corresponding predicted crack initiation lives (N_i) are given below.

Following are constants for the Basquin-Coffin Manson equation for material under consideration. These have been evaluated from classical LCF test as per ASTM standard.

Fatigue Strength coefficient σ_f = 586.06 MPa Fatigue ductility coefficient ε_f = 0.2406
Elastic modulus E = 200 GPa , Exponent of R-O equation m = 0.1837516
Exponents of Basquin-Coffin Manson Equation b = -0.0757, c = -0.4814,

1. Basquin-Coffin Manson equation – This is the classical strain-life equation, which predicts the number of cycle to fail under applied strain range only.

$$\frac{\Delta\varepsilon}{2} = \frac{\sigma_f'}{E}(2N)^b + \varepsilon_f'(2N)^c$$

Number of cycles to initiate the crack N_i = 370

2. To consider the mean stress effect Morrow (1968) modified the strain -life equation and account it in the elastic term only of the strain-life equation as-

$$\frac{\Delta\varepsilon}{2} = \frac{(\sigma_f' - \sigma_m)}{E}(2N)^b + \varepsilon_f'(2N)^c$$

Number of cycles to initiate the crack N_i = 331

Above equation predicts that the ratio of elastic to plastic strain is dependent on mean stress, which is not true from the materials constitutive relations.

3. Further Manson and Halford (1981) modified the strain-life equation to maintain the independence of the elastic-plastic strain ratio from mean stress and the modified equation is-

$$\frac{\Delta\varepsilon}{2} = \frac{\left(\sigma_f^{'} - \sigma_m\right)}{E}\left(2N\right)^b + \varepsilon_f^{'}\left(\frac{\sigma_f^{'} - \sigma_m}{\sigma_f^{'}}\right)^{\frac{c}{b}}\left(2N\right)^c$$ Number of cycles to initiate the crack $N_i = 15$

4. Smith, Watson, and Topper (1970) has suggested a SWT Parameter that is the product $\sigma_{max}\varepsilon_a$ is assumed to control the life, where of course $\sigma_{max} = \sigma_m + \sigma_a$. A life equation is obtained by noting that $\sigma_{max}\varepsilon_a = \sigma_a\varepsilon_a$ if the mean stress is zero and the strain-life equation as-

$$\sigma_{max}\frac{\Delta\varepsilon}{2} = \frac{\left(\sigma_f^{'}\right)^2}{E}\left(2N\right)^b + \sigma_f^{'}\varepsilon_f^{'}\left(2N\right)^c$$ Number of cycles to initiate the crack $N_i = 178$

5. In case of ratcheting-fatigue interaction, accumulation of ratcheting strain exhausts the ductility and hence fails in less number of cycles (detail discuss is in section 5.0). To account for the effect of ratcheting strain on fatigue life further, it was deducted from fatigue ductility coefficient in the classical strain-life equation as-

$$\frac{\Delta\varepsilon}{2} = \frac{\sigma_f^{'}}{E}\left(2N\right)^b + \left(\varepsilon_f^{'} - \varepsilon_r\right)\left(2N\right)^c$$ Number of cycles to initiate the crack $N_i = 132$

6. When account the ratcheting strain effect along with Morrow's modification, the strain-life equation becomes as-

$$\frac{\Delta\varepsilon}{2} = \frac{\left(\sigma_f^{'} - \sigma_m\right)}{E}\left(2N\right)^b + \left(\varepsilon_f^{'} - \varepsilon_r\right)\left(2N\right)^c$$ Number of cycles to initiate the crack $N_i = 118$

7. When account the ratcheting strain effect along with Manson and Halford 's modification, the strain-life equation becomes–

$$\frac{\Delta\varepsilon}{2} = \frac{\left(\sigma_f^{'} - \sigma_m\right)}{E}\left(2N\right)^b + \left(\varepsilon_f^{'} - \varepsilon_r\right)\left(\frac{\sigma_f^{'} - \sigma_m}{\sigma_f^{'}}\right)^{\frac{c}{b}}\left(2N\right)^c$$ Number of cycles to initiate the crack $N_i = 12$

The above study shows that none of the above strain-life equation except Manson and Halford with ratchet strain modification gives reasonable accurate number of cycles. It is noted that the strain/stress data used in above calculation are based on FE analysis with unstabilised (monotonic) material strain curve with multi-linear kinematic hardening rule which over predicts the ratchet strains as well as strain range. In view of this from the above study, it can be interpreted that Manson and Halford's modified strain-life equation along with ratchet strain is considered to be close to the experimental crack initiation cycles and it accounts for the non-relaxing mean stress (due to pressure load) and accumulated ratchet strain which are important to evaluate fatigue life for ratcheting-fatigue interaction.

5 UNIAXIAL FATIGUE RATCHETING TESTS ON ROUND LCF SPECIMENS

In all these tests, there was significant accumulation of ratchet strain over a number of applied cycles along with presence of non-relaxing internal pressure stress and led to very early fatigue crack initiation in the component (Table 2). In view of this, it is instructive to address the influence of ratcheting strain and non-relaxing pressure stress on fatigue behaviour. To understand the phenomena, a series of uniaxial ratcheting-fatigue experiments at specimen level have been performed.

These tests loading were given in two blocks. In first loading block of 100 cycles, i.e. uniaxial stress controlled ratcheting tests, various combinations of mean stress and stress amplitude was applied. Stress amplitude was kept small so that the hysteresis loop will not open (insignificant plastic strain range) and there would be insignificant fatigue damage in 100 cycles. It was observed that ratcheting strain accumulation rate saturates well before 100 cycles for all the applied loadings combinations. Further on the same pre-ratcheted specimens, second loading block of strain controlled, i.e. LCF tests, ±1.0% strain amplitude were applied. The ±1.0% strain amplitude was selected since in some of the ratcheting-fatigue tests on elbow, the strain range at crown location was found to be nearly 2%. In addition to this, few fresh specimens were also tested with ±1.0% strain amplitude loading to obtain base line LCF life of material in

order to understand and quantify the loss of LCF life in the pre ratchet specimen test. All the tests were continued until fracture and the LCF life was defined when there is 10% drop in the load.

Fig.13 shows the comparing of the LCF life of fresh specimen that is, without any pre-ratcheting deformation with that of different pre-ratcheting deformated specimens. Here also, similar to pipe-elbow ratcheting tests, it is observed that presence of ratcheting strain reduces the fatigue life. In this investigation a maximum ratcheting strain of about 8% has been observed in one of the test where the fatigue life has reduce to nearly half. This can be interpreted as the accumulation of plastic strain exhausts the ductility of material. Hence, in case of post ratchet LCF tests, the material has reduced ductility available and hence, failure occurs in less number of cycles of same amplitude in comparison to fresh material.

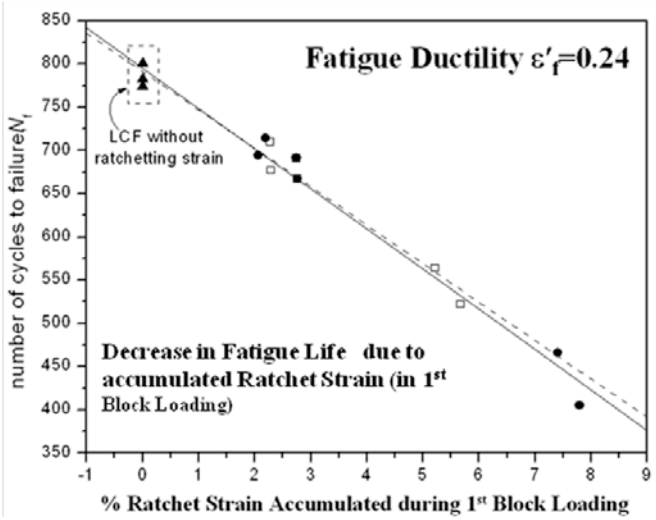

Figure13. Influence of accumulated ratcheting strain on the LCF life.

6 CONCLUSIONS

The present ratcheting-fatigue investigation on pipe-elbow assembly and uniaxial specimen has revealed following:

1. FE analyses have shown that transition of material constitutive behaviour from unstabilised (monotonic material σ-ε curve) to stabilised (cyclic σ-ε curve) takes some finite loading cycles. This has been revealed by the comparison of Load-LLD hysteresis for the two material conditions with test results. The 1st cycle response is closely simulated by the monotonic σ-ε curve while after the 10th or more cycles, the response is closely simulated by cyclic σ-ε curve.
2. The ratcheting-fatigue crack initiation in very few cycles (in comparison to LCF life) is primarily due to the presence of non-relaxing mean stress (due to pressure load) and ductility exhaustion as result of accumulating ratchet strain. Hence these must be accounted in the LCF calculations. The uniaxial ratcheting tests have revealed that accumulation of plastic strain exhausts the ductility of material and hence, specimens fails in less number of cycles of same amplitude in comparison to fresh material. The crack initiation study shows that none of the strain-life equation except Manson and Halford (1981) with ratchet strain modification gives reasonable accurate number of cycles for crack initiation.
3. In most of the elbow tests, for the applied combination of pressure and displacement controlled loading, equivalent pseudo linear stress amplitude (as per ASME Section III equation 9 with B'_2 index) is much larger then 3Sm limit and still the failure took place in significant number of cycles which is much more than in one earthquake. Therefore, it can be concluded that current ASME design rule provides adequate safety margin against the ratcheting-fatigue failure of pressurized elbow during the seismic loading.

Acknowledgement

The authors gratefully acknowledge the contribution of Prof. Amitab De of IIT- Bombay, Mumbai in active planning of whole ratchteing-fatigue test series and providing test facility for the same. The authors also gratefully acknowledge Dr. Shivaprasad and Dr. S. Tarafder of NML, Jamshedpur in conducting the

uniaxial fatigue ratcheting tests and investigations. The authors also gratefully acknowledge Mr. Puneet Arora, Mr. M A Khan, Mr. Sunil Satpute, Mr. S N Bodle, Mr. Nandanwar, Mr. Jagtap of RSD, BARC; Mr. J. L. Singh, Mr. Nitin Kumar of PIED, BARC and Mr. Anukumar, Mr. Mehta of CnID, BARC, for carrying out instrumentation and collecting the valuable data / information during the ratcheting-fatigue tests on pipe-elbow assembly.

REFERENCES

Bari, S., Hassan, T. 2000. Anatomy of coupled constitutive models for ratcheting simulation. International Journal of Plasticity. Vol. 16. P. 381-409.

Boussaa D., Van, K. D., Labbe, P., Tang, H. T. 1994. Fatigue–Seismic Ratcheting Interactions in pressurized Elbows. Journal of Pressure Vessel Technology. Vol. 116. P. 396-402.

Chaboche, J. L., 1991. On some modifications of kinematic hardening to improve the description of ratcheting effects. Int. J. Plasticity. Vol. 7. P. 661–678.

Hassan, T., Kyriakides, S., 1992. Ratcheting in cyclic plasticity, Part I: uniaxial behavior. Int. J. Plasticity. Vol. 8. P. 91–116.

Lin, Chu. 2000. Mean stress effects on low cycle fatigue for a precipitation hardened martensitic stainless steel in different tempers. Fat Fract Engg Mater Struct. Vol. 23. P. 545-553.

Manson, S. S. and Halford, G. R. 1981. Practical implementation of the double linear damage rule and damage curve approach for treating cumulative damage. Int. Jour. Fract. Vol. 17. P. 169-172.

Morrow, J. 1968. Fatigue properties of metals. In: Fatigue Design Handbook, Section 3.2, ed. J. A. Graham, Society of Automotive Engineers, Warrendale, PA, Vol. AE-4.

Ohno, N., Kachi, Y., 1986. A constitutive model of cyclic plasticity for nonlinear hardening materials. J. Appl. Mech. Vol. 53. P. 395–403.

Rahman, S. M., Hassan, T., Edmundo, C. 2008. Evaluation of cyclic plasticity models in ratcheting simulation of straight pipes under cyclic bending and steady internal pressure. International Journal of Plasticity. Vol. 24. P. 1756–1791.

Smith, K. N., Watson, P. and Topper, T. H. 1970. A stress-strain function for the fatigue of metals. J. Mater. ASTM. Vol. 5(4). P. 767-778.

Touble, F., Baly, N. and Lacire, M. H. 1999. Experimental, Analytical and regulatory evaluation of seismic behaviour of piping system. ASME journal of Pressure Vessel Technology. Vol. 121. P. 388-392.

Weib, E., Postberg, B., Nicak, T. and Rudolph, J. 2004. Simulation of ratcheting and low cycle fatigue. International Journal of pressure vessel and piping. Vol. 81. P. 235-241.

Xia, Z., Kujawski, D. and Ellyin, F. 1996. Effect of mean stress and ratcheting strain on fatigue life of steel. Int J Fatigue. Vol. 18. P. 335-341.

Yahiaoui, K., Moffat, D. G. and Moreton, D. N. 1996. Pressurised piping elbows under simulated seismic bending: design code implications. Proc. Instn Mech Engrs. Vol-210.